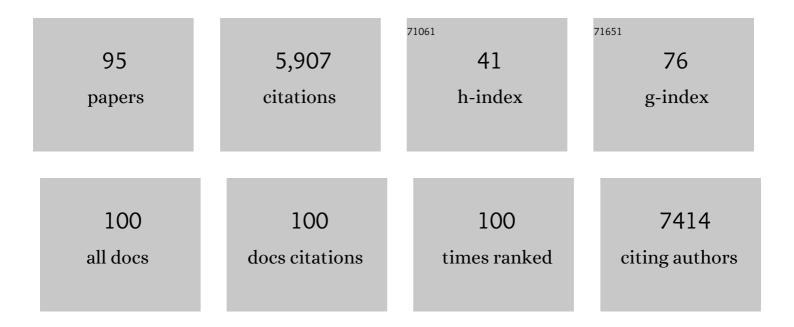
## Roger Wepf

List of Publications by Year in descending order

Source: https://exaly.com/author-pdf/8235922/publications.pdf Version: 2024-02-01



ROCEP WEDE

#	Article	IF	CITATIONS
1	Surface layer of Ptâ€O e bonds on CeO x nanowire with high ORR activity converted by proton beam irradiation. Journal of the American Ceramic Society, 2021, 104, 1945-1952.	1.9	6
2	Fluorescence-guided lamella fabrication with ENZEL, an integrated cryogenic CLEM solution for the cryo-electron tomography workflow. Microscopy and Microanalysis, 2021, 27, 3234-3235.	0.2	1
3	ENZEL - A cryogenic, retrofittable, coincident fluorescence, electron, and ion beam solution for the cryo-electron tomography workflow Microscopy and Microanalysis, 2021, 27, 3228-3229.	0.2	2
4	Can one determine the density of an individual synthetic macromolecule?. Soft Matter, 2019, 15, 6547-6556.	1.2	0
5	Correlative UHV-Cryo Transfer Suite: Connecting Atom Probe, SEM-FIB, Transmission Electron Microscopy via an Environmentally-Controlled Glovebox. Microscopy and Microanalysis, 2019, 25, 2494-2495.	0.2	4
6	OMNY—A tOMography Nano crYo stage. Review of Scientific Instruments, 2018, 89, 043706.	0.6	48
7	Robust workflow and instrumentation for cryo-focused ion beam milling of samples for electron cryotomography. Ultramicroscopy, 2018, 190, 1-11.	0.8	68
8	In Situ Techniques for Developing Robust Li–S Batteries. Small Methods, 2018, 2, 1800133.	4.6	41
9	Correlation of live-cell imaging with volume scanning electron microscopy. Methods in Cell Biology, 2017, 140, 123-148.	0.5	8
10	Direct observation of individual hydrogen atoms at trapping sites in a ferritic steel. Science, 2017, 355, 1196-1199.	6.0	224
11	Enabling Atom Probe Analyses of New Materials Classes with Vacuum-Cryo-Transfer Capabilities. Microscopy and Microanalysis, 2017, 23, 612-613.	0.2	11
12	OMNY PIN—A versatile sample holder for tomographic measurements at room and cryogenic temperatures. Review of Scientific Instruments, 2017, 88, 113701.	0.6	44
13	Addendum to "Three-dimensional mass density mapping of cellular ultrastructure by ptychographic X-ray nanotomography―[J. Struct. Biol. 192 (2015) 461–469]. Journal of Structural Biology, 2016, 193, 83.	1.3	2
14	A Versatile High-Vacuum Cryo-transfer System for Cryo-microscopy and Analytics. Biophysical Journal, 2016, 110, 758-765.	0.2	13
15	Methods in Creating, Transferring, & Measuring Cryogenic Samples for APT. Microscopy and Microanalysis, 2015, 21, 517-518.	0.2	23
16	The ultrastructure of fibronectin fibers pulled from a protein monolayer at the air-liquid interface and the mechanism of the sheet-to-fiber transition. Biomaterials, 2015, 36, 66-79.	5.7	14
17	Three-dimensional mass density mapping of cellular ultrastructure by ptychographic X-ray nanotomography. Journal of Structural Biology, 2015, 192, 461-469.	1.3	72
18	Macromolecular 3D SEM reconstruction strategies: Signal to noise ratio and resolution. Ultramicroscopy, 2014, 144, 43-49.	0.8	4

#	Article	IF	CITATIONS
19	Correlative 3D Imaging: CLSM and FIB-SEM Tomography Using High-Pressure Frozen, Freeze-Substituted Biological Samples. Methods in Molecular Biology, 2014, 1117, 593-616.	0.4	16
20	Phase-contrast imaging in aberration-corrected scanning transmission electron microscopy. Micron, 2013, 49, 1-14.	1.1	19
21	Mechanisms of haptoglobin protection against hemoglobin peroxidation triggered endothelial damage. Cell Death and Differentiation, 2013, 20, 1569-1579.	5.0	65
22	Threeâ€dimensional pore structure and ion conductivity of porous ceramic diaphragms. AICHE Journal, 2013, 59, 1446-1457.	1.8	52
23	Freezing Continuous-Flow Self-Assembly in a Microfluidic Device: Toward Imaging of Liposome Formation. Langmuir, 2013, 29, 1717-1723.	1.6	37
24	Simultaneous Correlative Scanning Electron and High-NA Fluorescence Microscopy. PLoS ONE, 2013, 8, e55707.	1.1	95
25	The Mechanism of Toxicity in HET-S/HET-s Prion Incompatibility. PLoS Biology, 2012, 10, e1001451.	2.6	123
26	The structure of dodecagonal (Ta,V)1.6Te imaged by phase-contrast scanning transmission electron microscopy. Journal of Solid State Chemistry, 2012, 194, 106-112.	1.4	3
27	Bridging Microscopes. Methods in Cell Biology, 2012, 111, 325-356.	0.5	62
28	Characterization of Catalysts in an Aberration-Corrected Scanning Transmission Electron Microscope. Journal of Physical Chemistry C, 2011, 115, 1080-1083.	1.5	33
29	Height and Width of Adsorbed Dendronized Polymers: Electron and Atomic Force Microscopy of Homologous Series. Macromolecules, 2011, 44, 6785-6792.	2.2	46
30	Measuring single-nanoparticle wetting properties by freeze-fracture shadow-casting cryo-scanning electron microscopy. Nature Communications, 2011, 2, 438.	5.8	159
31	3D geometry and topology of pore pathways in Opalinus clay: Implications for mass transport. Applied Clay Science, 2011, 52, 85-95.	2.6	190
32	Serial FIB/SEM imaging for quantitative 3D assessment of the osteocyte lacuno-canalicular network. Bone, 2011, 49, 304-311.	1.4	123
33	Phase tomography from x-ray coherent diffractive imaging projections. Optics Express, 2011, 19, 21345.	1.7	183
34	On the application of focused ion beam nanotomography in characterizing the 3D pore space geometry of Opalinus clay. Physics and Chemistry of the Earth, 2011, 36, 1539-1544.	1.2	75
35	Focussed ion beam nanotomography reveals the 3D morphology of different solid phases in hardened cement pastes. Journal of Microscopy, 2011, 241, 234-242.	0.8	24
36	Minimization of amorphous layer in Ar+ ion milling for UHR-EM. Ultramicroscopy, 2011, 111, 1224-1232.	0.8	23

#	Article	IF	CITATIONS
37	The Largest Synthetic Structure with Molecular Precision: Towards a Molecular Object. Angewandte Chemie - International Edition, 2011, 50, 737-740.	7.2	111
38	Three-dimensional reconstruction of Heterocapsa circularisquama RNA virus by electron cryo-microscopy. Journal of General Virology, 2011, 92, 1960-1970.	1.3	12
39	Ptychographic X-ray computed tomography at the nanoscale. Nature, 2010, 467, 436-439.	13.7	766
40	Towards quantitative 3D imaging of the osteocyte lacuno-canalicular network. Bone, 2010, 47, 848-858.	1.4	139
41	3D-microstructure analysis of hydrated bentonite with cryo-stabilized pore water. Applied Clay Science, 2010, 47, 330-342.	2.6	84
42	Threeâ€dimensional reconstruction of biological macromolecular complexes from inâ€lens scanning electron micrographs. Journal of Microscopy, 2009, 234, 287-292.	0.8	13
43	A strategy for correlative microscopy of large skin samples: towards a holistic view of axillary skin complexity. Experimental Dermatology, 2008, 17, 73-81.	1.4	14
44	Correlative 3D Microscopy: CLSM and FIB/SEM Tomography. Imaging & Microscopy, 2008, 10, 30-31.	0.1	4
45	Assessing the risk of skin damage due to femtosecond laser irradiation. Journal of Biophotonics, 2008, 1, 470-477.	1.1	50
46	Influence of pH on colloidal properties and surface activity of polyglycerol fatty acid ester vesicles. Journal of Colloid and Interface Science, 2008, 327, 446-450.	5.0	22
47	Visualizing nuclei in skin cryosections: viable options to 46-diamidino-2-phenylindol for confocal laser microscopy. Skin Research and Technology, 2008, 14, 324-326.	0.8	4
48	Risk estimation of skin damage due to ultrashort pulsed, focused near-infrared laser irradiation at 800â€,nm. Journal of Biomedical Optics, 2008, 13, 041320.	1.4	57
49	Life-Like Physical Fixation of Large Samples for Correlative Microscopy. Microscopy and Microanalysis, 2008, 14, 680-681.	0.2	0
50	Life-like physical fixation of large samples for correlative microscopy. , 2008, , 351-352.		0
51	Correlative 3D microscopy: CLSM and FIB/SEM tomography used to study cellular entry of vaccinia virus. , 2008, , 361-362.		2
52	Nanoparticles – An efficient carrier for drug delivery into the hair follicles. European Journal of Pharmaceutics and Biopharmaceutics, 2007, 66, 159-164.	2.0	488
53	Pros and cons: cryo-electron microscopic evaluation of block faces versus cryo-sections from frozen-hydrated skin specimens prepared by different techniques. Journal of Microscopy, 2007, 225, 201-207.	0.8	21
54	Cryoâ€FIBâ€nanotomography for quantitative analysis of particle structures in cement suspensions. Journal of Microscopy, 2007, 227, 216-228.	0.8	54

#	Article	IF	CITATIONS
55	Skin imaged by femtosecond laser irradiation: a risk assessment for in vivo applications. , 2006, 6191, 36.		5
56	Improved Native Tissue Ultrastructure Investigations by High Pressure Freezing and Cryo-SEM. Microscopy and Microanalysis, 2006, 12, 1114-1115.	0.2	0
57	Investigation of differences in follicular penetration of particle-and nonparticle-containing emulsions by laser scanning microscopy. Laser Physics, 2006, 16, 747-750.	0.6	44
58	Are Sweat Glands an Alternate Penetration Pathway? Understanding the Morphological Complexity of the Axillary Sweat Gland Apparatus. Skin Pharmacology and Physiology, 2006, 19, 38-49.	1.1	47
59	Structural investigations of human hairs by spectrally resolved ellipsometry. Journal of Biomedical Optics, 2006, 11, 014029.	1.4	3
60	Noninvasive measurement of cell volume changes by negative staining. Journal of Biomedical Optics, 2005, 10, 064017.	1.4	13
61	Sealing the live part of the skin: The integrated meshwork of desmosomes, tight junctions and curvilinear ridge structures in the cells of the uppermost granular layer of the human epidermis. European Journal of Cell Biology, 2004, 83, 655-665.	1.6	71
62	Dead but Highly Dynamic – The Stratum corneum Is Divided into Three Hydration Zones. Skin Pharmacology and Physiology, 2004, 17, 246-257.	1.1	91
63	Characterization of multiphoton laser scanning device optical parameters for image restoration. , 2004, , .		3
64	Improvements for HR- and Cryo-SEM by the VCT 100 High-Vacuum Cryo Transfer System and SEM Cooling Stage. Microscopy and Microanalysis, 2004, 10, 970-971.	0.2	6
65	A cryogenic scanning force microscope for the characterization of frozen biological samples. Applied Physics A: Materials Science and Processing, 2003, 76, 893-898.	1.1	2
66	From tissue to cellular ultrastructure: closing the gap between micro- and nanostructural imaging. Journal of Microscopy, 2003, 212, 91-99.	0.8	72
67	Cryopreparation of skin samples: A comparison between ultrathin cryosections and resin embedded sections of human skin. Microscopy and Microanalysis, 2003, 9, 180-181.	0.2	1
68	No compromise in correlative microscopy: One sample, one preparation protocol for CLSM and TEM. Microscopy and Microanalysis, 2003, 9, 1198-1199.	0.2	0
69	Topographic Measurements of Real Structures in reflection Confocal Laser Scanning Microscope (CLSM). Microscopy and Microanalysis, 2003, 9, 162-163.	0.2	4
70	Combining histological and ultrastructural description of high-pressure frozen skin samples by correlative CLSM and TEM. Microscopy and Microanalysis, 2003, 9, 374-375.	0.2	0
71	Improving image storage and access in an integrated microscopy unit: experiences with a commercial image database system. Microscopy and Microanalysis, 2003, 9, 530-531.	0.2	0
72	Publisher's Note: Hydration dynamics of human fingernails: An ellipsometric study [Phys. Rev. E65, 061913 (2002)]. Physical Review E, 2002, 66, .	0.8	0

#	Article	IF	CITATIONS
73	Hydration dynamics of human fingernails: An ellipsometric study. Physical Review E, 2002, 65, 061913.	0.8	17
74	Distribution of sunscreens on skin. Advanced Drug Delivery Reviews, 2002, 54, S157-S163.	6.6	250
75	Investigation of the swelling of human skin cells in liquid media by tapping mode scanning force microscopy. Applied Physics A: Materials Science and Processing, 2001, 72, S125-S128.	1.1	39
76	Localization of Ceramide and Glucosylceramide in Human Epidermis by Immunogold Electron Microscopy. Journal of Investigative Dermatology, 2001, 117, 1126-1136.	0.3	67
77	Mouse anti-ceramide antiserum: a specific tool for the detection of endogenous ceramide. Glycobiology, 2001, 11, 451-457.	1.3	40
78	Structure and Assembly of Intracellular Mature Vaccinia Virus: Isolated-Particle Analysis. Journal of Virology, 2001, 75, 11034-11055.	1.5	55
79	The Human Stratum corneum Layer: An Effective Barrier against Dermal Uptake of Different Forms of Topically Applied Micronised Titanium Dioxide. Skin Pharmacology and Physiology, 2001, 14, 92-97.	1.1	143
80	High-Pressure Freezing Provides New Information on Human Epidermis: Simultaneous Protein Antigen and Lamellar Lipid Structure Preservation. Study on Human Epidermis by Cryoimmobilization. Journal of Investigative Dermatology, 2000, 114, 1030-1038.	0.3	62
81	Penetration pathways of fluorescent dyes in human hair fibres investigated by scanning near-field optical microscopy. Journal of Microscopy, 2000, 200, 179-186.	0.8	27
82	Entry of the Two Infectious Forms of Vaccinia Virus at the Plasma Membane Is Signaling-Dependent for the IMV but Not the EEV. Molecular Biology of the Cell, 2000, 11, 2497-2511.	0.9	162
83	A Versatile High-Vacuum Cryo-Transfer for Cryo-FESEM, Cryo-SPM and other Imaging Techniques. Microscopy and Microanalysis, 1999, 5, 424-425.	0.2	8
84	Quantification of total calcium in terminal cisternae of skinned muscle fibers by imaging electron energy-loss spectroscopy. Journal of Muscle Research and Cell Motility, 1999, 20, 505-515.	0.9	3
85	Title is missing!. International Journal of Cosmetic Science, 1999, 21, 399-411.	1.2	25
86	TEM moiré patterns explain STM images of bacteriophage T5 tails. Ultramicroscopy, 1997, 69, 129-137.	0.8	12
87	Nic96p is required for nuclear pore formation and functionally interacts with a novel nucleoporin, Nup188p Journal of Cell Biology, 1996, 133, 1141-1152.	2.3	99
88	Rab8 promotes polarized membrane transport through reorganization of actin and microtubules in fibroblasts Journal of Cell Biology, 1996, 135, 153-167.	2.3	228
89	Roles for Rac1 and Cdc42 in planar polarization and hair outgrowth in the wing of Drosophila Journal of Cell Biology, 1996, 135, 1277-1289.	2.3	203
90	The Surface Structure of Biomolecules Using Correlative Microscopy: TEM, SEM, STM and AFM. Proceedings Annual Meeting Electron Microscopy Society of America, 1996, 54, 314-315.	0.0	0

#	Article	IF	CITATIONS
91	The core of the mammalian centriole contains $\hat{I}^3$ -tubulin. Current Biology, 1995, 5, 1384-1393.	1.8	110
92	A novel nuclear pore protein Nup133p with distinct roles in poly(A)+ RNA transport and nuclear pore distribution. EMBO Journal, 1994, 13, 6062-75.	3.5	143
93	Platinum/iridium/carbon: a highâ€resolution shadowing material for TEM, STM and SEM of biological macromolecular structures. Journal of Microscopy, 1991, 163, 51-64.	0.8	49
94	STM of freeze-dried and Ptî—,Irî—,C-coated bacteriophage T4 polyheads. Journal of Structural Biology, 1989, 102, 170-177.	0.9	22
95	Active Pt-Nanocoated Layer with Pt–O–Ce Bonds on a CeO <sub><i>x</i></sub> Nanowire Cathode Formed by Electron Beam Irradiation. ACS Omega, 0, , .	1.6	2